J. H. LIENHARD
Professor. Mem. ASME

V. K. DHIR
Research Associate. Assoc. Mem. ASME

D. M. RIHERD
Whirlpool Fellow. Student Mem. ASME

Boiling and Phase Change Laboratory,
Mechanical Engineering Department,
University of Kentucky,
Lexington, Ky.

Peak Pool Boiling Heat-Flux Measurements on Finite Horizontal Flat Plates[1]

Experimental data obtained at both earth-normal and elevated gravity, in a variety of organic liquids and water, are used to verify the hydrodynamic theory for the peak pool boiling heat flux on flat plates. A modification of Zuber's formula, which gives a 14 percent higher peak heat flux, is verified as long as the flat plate is more than three Taylor wavelengths across. For smaller heaters, the hydrodynamic theory requires a wide variation in heat flux owing to discontinuities in the number of escaping jets. Data for smaller plates bear out this predicted variation with heat fluxes that range between 40 percent and 235 percent of Zuber's predicted value. Finally, a method is suggested for augmenting the peak heat flux on large heaters, and shown experimentally to be viable.

Introduction

THE AIM of this study is to provide experimental verification of predictions of the peak heat flux, q_{max}, on horizontal flat plate heaters of *finite* extent.

There has existed for over two decades, a hydrodynamic theory of q_{max} for the *infinite* horizontal flat plate. This theory was given in a fully rationalized form by Zuber [1][2] in 1958 on the basis of a concept and correlation originally suggested by Kutateladze [2] ten years earlier. The now well-known Zuber-Kutateladze expression is[3]

$$q_{max_Z} \equiv \frac{\pi}{24} \rho_g^{1/4} h_{fg} \sqrt[4]{g\sigma(\rho_f - \rho_g)} \tag{1}$$

where, for reasons that will be clear in a moment, we identify this prediction as a particular property of the boiled liquid and designate it as q_{max_Z}.

In a very recent paper [3] we reexamined the derivation of equation (1) in the light of more recent experimental and theoretical findings (notably [4]). We argued that the Helmholtz unstable disturbance, which made the escaping vapor jets collapse and initiated the peak heat flux transition, was not the critical Rayleigh wave in the jet. It is, instead, the Taylor unstable wavelength which is carried into the jet from the horizontal liquid-vapor interface. The resulting expression for the peak heat flux on an infinite flat plate, q_{max_F}, was 14 percent higher than Zuber's. Thus

$$\frac{q_{max_F}}{q_{max_Z}} = 1.14 \tag{2}$$

Equation (2) is a special case of the general sort of correlation that applies to finite heaters (see e.g., [4, 5, 6, and 7])

$$\frac{q_{max}}{q_{max_Z}} = f(L'); \quad L' \equiv L\sqrt{g(\rho_f - \rho_g)/\sigma} \tag{3}$$

where, for infinite heaters, the influence of any characteristic length, L, must disappear.

q_{max_F} for Finite Flat Plates

The problem of verifying equation (2) lies in the fact that data cannot be obtained on infinite flat plate heaters. Whether or not equation (2) has any utility will depend heavily on whether or not, and to what extent, finite plates approximate infinite plates.

Fig. 1 illustrates three kinds of flat plate heaters. Fig. 1(*a*) is the infinite plate thought-model. Fig. 1(*b*) is the logical approximation to the infinite plate. It contains a finite number of jets spaced (in accordance with the hydrodynamic theory) on the most susceptible Taylor wavelength, λ_d. It has vertical side walls located one-half a wavelength from the center line of the outer jets in the grid. We know of no experiments which reflect this configuration exactly. Only two sets of data in the literature approach it. The classical data of Cichelli and Bonilla [8] are for the correct configuration—a 9-1/2-cm-dia disk heater which formed the bottom of the cylindrical container for the boiled liquid. But many of their data must be eliminated because they were obtained on "dirty" heaters. Most of the remainder are for nominal fluids of extremely low purity—actually

---

[1] This work received support from NASA Grant NGR-18-001-035, under the cognizance of the Lewis Research Center.

[2] Numbers in brackets designate References at end of paper.

[3] Symbols not defined in the text are ones in common use. They are explained in the Nomenclature.

Contributed by the Heat Transfer Division and presented at the Winter Annual Meeting, Detroit, Mich., November 11–15, 1973, of THE AMERICAN SOCIETY OF MECHANICAL ENGINEERS. Manuscript received by the Heat Transfer Division, February 12, 1973. Paper No. 73-WA/HT-30.

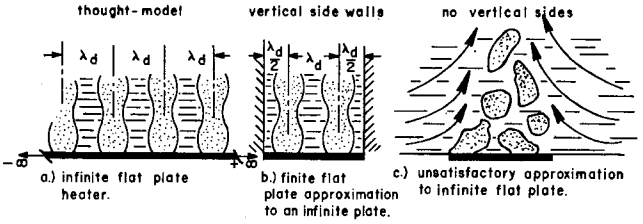

Fig. 1 Horizontal flat plate configurations, idealized and actual

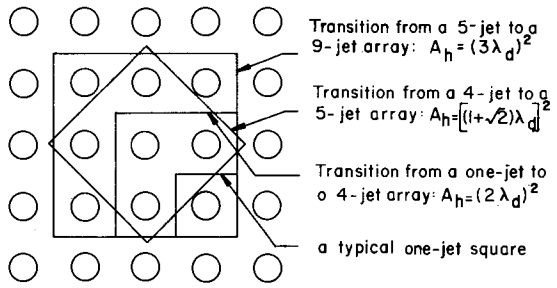

Fig. 2 Jet configurations on square heaters of various sizes

mixtures for which properties are not known and correlations cannot be applied. Only a few of their data for ethanol remain for use. Berenson [9] presented similar data for CCl_4 and n-pentane on 5 cm dia heaters that were subject to very close control of surface condition.

Fig. 1(c) shows another configuration for which there exist plenty of q_{max} data, none of which has much relation to the present "flat plate" configurations. This is the flat heater surrounded by a larger open bath of liquid. The peak heat flux in this configuration was shown in 1970 [10] to be strongly influenced by induced convection effects. These effects in turn required the inclusion of an additional parameter in equation (3), namely, the Borishanski number.

Since λ_d is on the order of two centimeters for most common liquids, a heater must be larger than most laboratory heaters before it includes "many" jets. If the heater area, A_H, does not correspond with an integral or large number of "cells" of area λ_d^2, then the heat flux will be determined by the actual number of jets on the plate, N_j. Thus

$$\frac{q_{max_{finite}}}{q_{max_Z}} = 1.14 \frac{N_j}{A_H/\lambda_d^2} \tag{4}$$

The problem of counting the number of jets on a finite plate is a little tricky. Fig. 2 shows how we would expect jets to be distributed on square plates of various sizes. If we suppose that no jet lies closer than $\lambda_d/4$ to the vertical side walls (except when $A_H < \lambda_d^2$), then transitions from 1 to 4 jets, from 4 to 5 jets, and from 5 to 9 jets will probably occur at $A_H = (2\lambda_d)^2$, $A_H = (1 + \sqrt{2})^2\lambda_d^2$, and $A_H = (3\lambda_d)^2$, respectively.

Proceding in this way and using equation (4), we can construct a sawtooth plot of q_{max} against heater size. This has been done in Fig. 3. Here we use the coordinates, q_{max}/q_{max_Z}, and heater width divided by λ_d (or $L'/2\pi\sqrt{3}$), as suggested by equation (3) where, for a plane interface,

$$\lambda_d = 2\pi\sqrt{3\sigma/g(\rho_f - \rho_g)}. \tag{5}$$

Curves consistent with equation (4) have been drawn in for N_j = 1, 4; 5, 9, ... For $N_j > 1$, only the portion below the line is strictly consistent with the model described in the foregoing. However, it is possible for the jets to locate themselves differently than shown in Fig. 2, particularly as N_j becomes larger. Thus we have arbitrarily extended each curve (for $N_j \geq 5$) to the left until the preceding curve is also above q_{max}/q_{max_Z}.

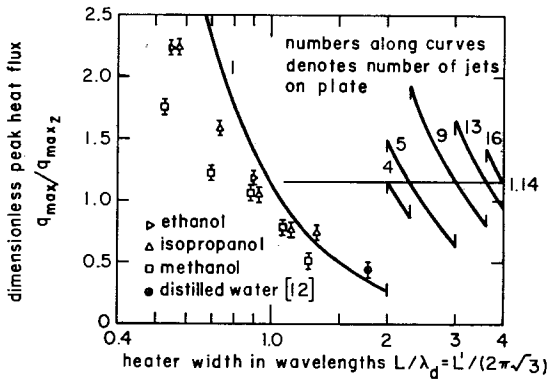

Fig. 3 Peak heat flux on a square finite flat plate with vertical side walls

It should be emphasized that only the curve for $N_j = 1$, and possibly for $N_j = 2$, have real theoretical validity. For the larger N_j's, not only are we unsure of the exact arrangement of jets, but minor variations of the true wavelength about λ_d can actually displace the lines. Thus while equation (4) is valid, the curves drawn on the right-hand side of Fig. 3 (and later in the paper, Fig. 9) should be taken as qualitative indications of behavior. That the curves are double-valued is also no serious objection. This implies simply that data might lie on one curve or the other.

The resulting curves deviate widely from $q_{max}/q_{max_Z} = 1.14$ on the left-hand side, and as L/λ_d is carried to larger and larger values, the deviations will become smaller and smaller. Thus equation (4) will reduce to equation (2) in the limit of large L'. Similar sets of curves can be built for heaters of other shapes. The use of semilogarithmic coordinates in Fig. 3 (and later in Fig. 9) is not implied by the theory, but is simply a convenience in presenting the material.

Experiments

We now need data with which to check equation (2), and its modification for small plates, equation (4). Two experiments

Nomenclature

A_H = area of heater

g, g_e = acceleration of gravity (subscript, e, denotes earth-normal gravity)

h_{fg} = latent heat of vaporization

L = a characteristic length (= width of a square heater or diameter of a circular heater, depending on context)

$L' = L\sqrt{g(\rho_f - \rho_g)/\sigma}$, a dimensionless heater size

N_j = number of escaping vapor jets on a heater of area, A_H

$q_{max}, q_{max_F}, q_{max_Z}$ = peak pool boiling heat flux. Subscript, F, denotes infinite flat plate value. Subscript, Z, denotes Zuber's prediction of q_{max}. q_{max_Z} is viewed as a characteristic of the boiled liquid in this study

λ_d = most susceptible Taylor unstable wavelength in a horizontal liquid-vapor interface

ρ_f, ρ_g = density of saturated liquid and vapor, respectively

σ = surface tension between a liquid and its vapor

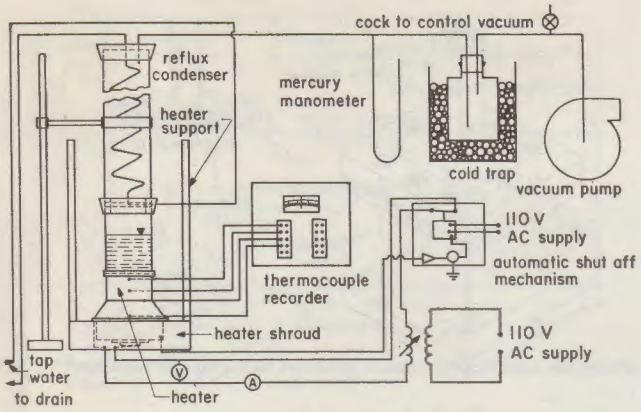

Fig. 4 Schematic diagram of stationary flat plate heater

will be described, one applicable to the range of larger L/λ_d's and one applicable to the smaller L/λ_d's.

Large L/λ_d Experiments. To reach large L/λ_d values we decided not just to make L (in this case the diameter of a circular heater) very large, but also to do experiments in which λ_d was very small. This was done by operating in a centrifuge, since $\lambda_d \sim g^{-1/2}$.

A detailed description of the flat plate apparatus that we developed is given in reference [11], and we shall only describe its major features here. The apparatus consisted of a heater, a heater support, an emergency shut-off mechanism, and a reflux condenser. This entire assembly was designed to operate either at earth-normal gravity or to be installed in Centrifuge Facility of the Boiling and Phase-Change Laboratory at the University of Kentucky.[4] A schematic diagram of the apparatus is shown in Fig. 4.

The heater itself was made of pure copper with a circular bell-shaped configuration. It has a diameter of 6.35 cm at the boiling surface, 10.16 cm at the butt end, and a height of 10.8 cm. A pyrex glass cylinder allowing a liquid head of about 6 cm sits on the heater surface and is held in place by two stainless steel flanges. Stainless steel has a much lower thermal conductivity than copper, hence the flanges have a very small cooling effect on the edges of the boiling surface.

Fig. 5 shows a sectioned view of the heater. Its lower portion consists of three rings wound with 4 m of 1.62-mm-dia nichrome wire, capable of dissipating 6 kw of power. Five iron-constantan thermocouples are positioned as shown in the figure to monitor the temperature in various parts of the heater body. The top two thermocouples were used to determine the heat flux to the boiling surface. A third thermocouple was used for a counter-check on the heat flux calculations and a fourth thermocouple to show whether steady-state conditions are reached.

The thermocouple in the base monitored the temperature for an electronic emergency shut-off system. This system cut off the power supply after the peak heat flux was reached. A cut-off system was necessary because the transition to film boiling effectively insulated the surface and permitted the temperature in the copper heater to run away. The shut-off system is fairly complex and full details are given in reference [11].

The flat plate heater accommodated more than three wavelengths for the alcohols, and about two for water, at earth-normal gravity, while these numbers increased as $g^{1/2}$ at higher gravities. The following reagent grade liquids were used: acetone (CH_3COCH_3), benzene (C_6H_6), isopropanol ($CH_3CHOHCH_3$), methanol (CH_3OH), and distilled water.

Elevated gravity tests were performed with the help of the centrifuge facility. Details of the centrifuge design are given in reference [7], and Fig. 6(*a*) shows the centrifuge facility. When

[4] We are grateful to Mr. Eugene Davis for his contributions to the design of this heater.

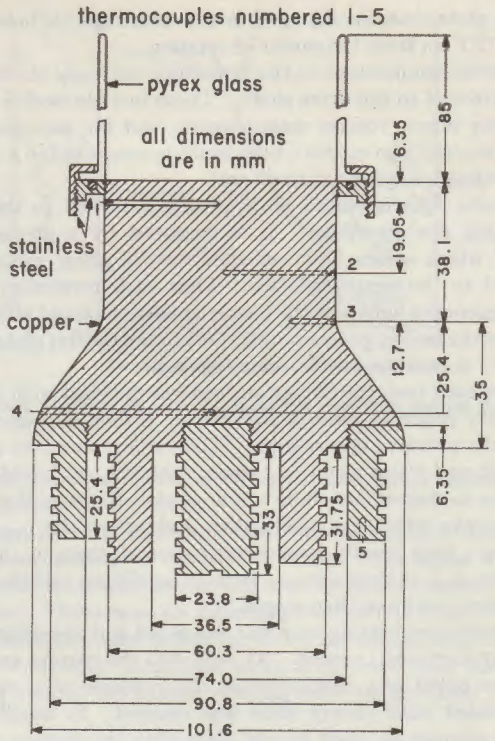

Fig. 5 Sectioned view of the flat plate heater

Fig. 6(*a*) Centrifuge facility—general view

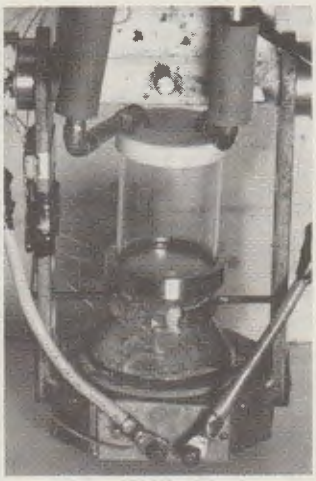

Fig. 6(*b*) Top view of flat-plate heater assembly installed at end of centrifuge arm

Fig. 6 Photographs of flat-plate apparatus and the centrifuge facility

the flat plate heater is mounted in the centrifuge, its boiling surface is 77.7 cm from the center of rotation.

Electrical connections to the centrifuge are made through slip rings attached to the drive shaft. Those include twelve circuits for power input, voltage measurement, and for thermocouples. The drive shaft also carries a tube which is connected to a vacuum pump through a rotary vacuum seal.

A strobe light is placed on a bracket attached to the stand supporting the centrifuge. It is triggered by a photoelectric pick-off which senses light reflected from a shiny metal piece attached to the centrifuge arm. Thus each revolution of the arm triggers the light and the heater appears to stand still so one can view the boiling process. Fig. 6(*b*) shows the flat plate heater assembly in position on the centrifuge arm.

Before each test, the boiling surface was polished with 220 grit size emery paper to remove any rust or carbon deposit formed during the previous observation. The surface was then cleaned with soap and warm water and rinsed with the test liquid. This was done to insure that there was no uncleanliness on the surface which might affect the wettability and affect the q_{max} data. Berenson's very careful experiments showed that, in this configuration, q_{max} is insensitive to surface conditions and that these precautions are more than ample.

The resistance heating wire was energized and the current was gradually increased in steps. At each step the current and voltage were noted and thermocouple observations were recorded and updated until steady state was reached. It usually took about 5 minutes to reach steady state after the current was increased to the next higher value.

Various regimes of nucleate boiling (e.g., the isolated bubble regime and the transition from single bubbles to slugs and columns) were easily discernible. The transition from nucleate to transitional boiling was identified by noting a slowdown of the boiling process and a sudden continuous increase in the thermocouple reading. The thermocouple reading kept on increasing for a while, even after the power was removed. In most cases, the power was cut off after visual observation of the boiling transition, rather than by triggering of the automatic shut-off mechanism.

The maximum probable error of the peak heat flux was estimated [11] as 7.7 percent. A few of the observations were repeated to check for reproducibility of results. Each time a new observation was made, the aforementioned procedure for cleaning the boiling surface was used and fresh test liquid was employed.

The flat plate test results are tabulated in Table 1 in both raw and reduced form.

Table 1 Peak heat flux data on 6.35-cm-dia circular flat plate heaters

Liquid	g/g_e	Pressure (k Pa)[a]	$\frac{L'}{2\pi\sqrt{3}}$	$q_{max} \times 10^{-6}$ $\left(\frac{W}{m^2}\right)$	$\frac{q_{max}}{q_{max_Z}}$
Acetone	1	98.58	3.71	3.94	1.18
	1	98.93	3.71	4.10	1.22
	4.97	23.99	7.69	3.44	1.14
	12.30	25.37	12.07	4.19	1.07
Benzene	4.97	18.06	7.36	2.98	1.21
	8.72	24.88	9.85	3.31	1.05
	17.5	27.09	14.07	4.19	1.07
Isopropanol	1	22.75	3.68	2.08	0.79
		46.53	3.78	3.34	1.00
		73.21	3.85	3.82	0.98
		88.52	3.88	4.54	1.10
		98.72	3.91	4.26	1.00
	4.97	18.06	8.20	5.39	1.51
Methanol	1	44.60	3.56	3.69	0.94
		47.43	3.56	4.13	1.02
		88.04	3.72	5.33	1.04
		96.38	3.75	5.33	1.01
		96.52	3.75	5.33	1.01
		98.10	3.75	5.33	1.00
Distilled water	1	14.48	2.24	3.34	0.70
		25.37	2.27	4.45	0.72
		29.51	2.28	4.26	0.66
		36.54	2.29	4.82	0.67
		39.16	2.29	4.54	0.62
		42.74	2.30	4.54	0.59

[a] 1 kiloPascal equals 101.97 kg/m² or 7.5006 torrs.

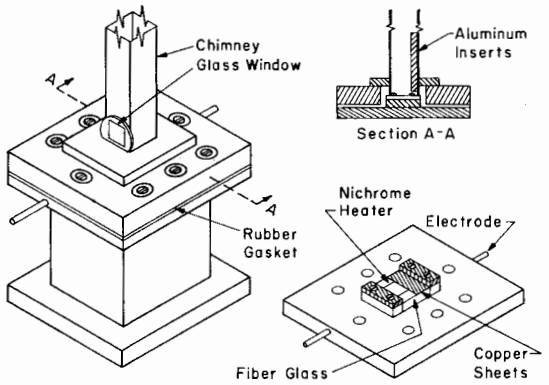

Fig. 7 Small plate heater apparatus

Small L/λ_d Experiments. The small L/λ_d apparatus is shown in Fig. 7. In this case, there was no advantage to working in the centrifuge since its purpose is only to increase L/λ_d by shrinking λ_d. Therefore a simple apparatus was made for stationary use only. It consists of a pair of electrodes positioned to accommodate nichrome resistance heater plates of varying width. Enough of each plate is short-circuited, as shown in the figure, so that the remaining active area is square. A chimney is fitted over the plate to contain the boiled liquid. Within the chimney are included spacers so the inside area of the chimney rises directly upward from the active heater area.

Table 2 Observations of q_{max} for finite horizontal square plates

Liquid	Width (cm)	Power (w)	$\frac{L}{\lambda_d}$	$\frac{q_{max}}{q_{max_Z}}$
Isopropanol	2.16	156	1.32	0.777
		148		0.738
		156		0.777
	1.52	102	0.93	1.021
		105		1.049
Methanol		132	0.89	1.048
		125		0.991
		127		1.010
		130		1.029
Ethanol		130	0.90	1.207
		130		1.207
		130		1.204
		119		1.103
Isopropanol	1.84	110	1.12	0.756
		108		0.743
		111		0.759
Methanol		146	1.07	0.789
		152		0.825
		147		0.800
Isopropanol	0.89	74	0.54	2.183
		80		2.354
		78		2.292
Methanol		74	0.52	1.726
		78		1.817
		74		1.726
Ethanol		80	0.33	2.178
		82		2.238
Methanol	1.21	100	0.70	1.266
		100		1.266
		100		1.266
Isopropanol		101	0.73	1.614
		94		1.506
		101		1.614
Methanol	2.16	118	1.26	0.467
		114		0.451
		110		0.435
		116		0.459

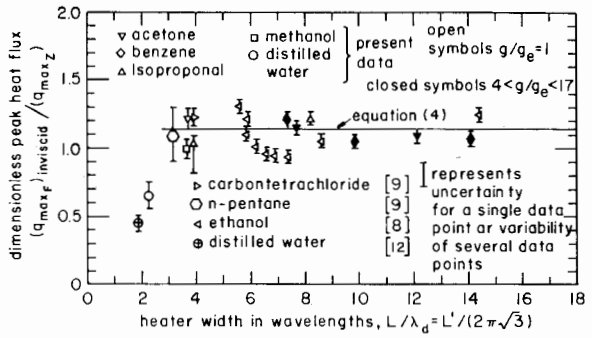

Fig. 8 Peak heat flux on broad flat-plate heaters with vertical side walls

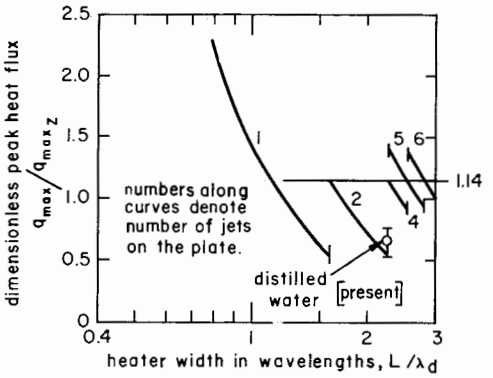

Fig. 9 Peak heat flux on a circular finite flat plate with vertical side walls

Each plate was washed with soap and warm water after it was installed, and then rinsed with the test liquid. This was done before each set of observations was made on the plate. The results of these observations are presented in both raw and reduced form in Table 2. The test liquids included reagent grade isopropanol and methanol, and 95 percent pure ethanol.

Discussion of Experimental Results

The available q_{max} data for $L/\lambda_d \geq 2$, from both this and other investigations, are plotted against L/λ_d (or $L'/2\pi\sqrt{3}$) in Fig. 8. Data for circular heaters (L = diameter) and one point for a square heater (reference [12], L = width) are included in the figure.

With reference to Fig. 8, we see that all the data are very closely represented by our version of Zuber's flat-plate prediction, equation (2), when L/λ_d exceeds about 3. The two data for smaller L/λ_d deviate sharply below the predicted value of $q_{max_F} = 1.14\ q_{max_Z}$, however. One of these data is our own for a circular heater. The other was obtained years ago by Costello [12] with a square heater.

In Fig. 3 we include Costello's data point along with our small L/λ_d data. This figure shows very clearly the effect of finite heater size on q_{max}. The data closely obey equation (4) for $N_j = 1$, between $L/\lambda_d = 1.0$ and 2.0, indicating that only one jet can be accommodated on the plate. This fact was substantiated by the scorch marks on the used plates. Circular marks, $\lambda_d/2$ in diameter, were observed repeatedly.

As the plate is shrunk to $L = \lambda_d/2$ we see that the data fall away from the curve. This is no surprise since the simple inviscid model no longer applies. The liquid return route is being squeezed into a viscous film crowded against the chimney, and considerations not included in the theory dictate q_{max}.

This result provides a dramatic verification of the hydrodynamic theory. It reveals a 5-fold variation of q_{max} which is accurately predicted by the theory until the theory breaks down owing to sidewall effects. It is, perhaps, ironic that Costello used the data point shown in the figure to support his own doubts as to the validity of the hydrodynamic theory.

Fig. 9 is a set of theoretical curves constructed for circular heaters in much the same way as those in Fig. 3 were constructed for square heaters. On this we include our own single data point for L/λ_d = diameter/λ_d = 2.3. This point, which actually represents 6 individual observations, touches the curve which corresponds to two jets on the heater.

A Scheme for Augmenting q_{max} on Large Plates

The fact that we can more than double q_{max} by closing in on the jets with vertical sidewalls suggests that it might be possible to augment q_{max} on large plates by building an "egg-crate" structure of vertical walls above a large plate.

We have built two such aluminum and brass structures to fit inside the glass cylinder shown above the copper heater in Fig. 6(*b*). The layout of these inserts is shown in Fig. 10. There was a clearance of about $^1/_2$ mm between the bottom of the egg crate and the heater surface. This avoided direct thermal contact with the heater surface.

The q_{max} data for stationary runs with the egg-crate structures in place are presented in Table 3. Data were taken with the liquid level both well above, and slightly below, the top of the structure. There was no difference in the resulting values of q_{max}. Since the walls of the egg crates have finite thickness, the heat flow directly under the walls is diverted into the unobstructed area of the heater and q_{max} must be increased to com-

Table 3 Peak heat flux for a large flat plate with an egg-crate structure above it

Egg-crate configuration	Liquid	Pressure kPa	q_{max} 10^5W/m²	q_{max}/q_{max_Z} based on total A_H	q_{max}/q_{max_Z} based on active A_H
L = 1.02 cm	Isopropanol	12.62	3.29	1.58	1.86
center to		12.62	3.29	1.58	1.86
center, made		15.23	3.40	1.52	1.80
of 0.81-mm		19.90	3.62	1.44	1.70
sheet alumi-			3.62	1.44	1.70
num			3.51	1.40	1.65
			3.51	1.40	1.65
	Acetone	36.64	4.05	1.70	2.01
L = 0.635 cm	Isopropanol	15.40	3.72	1.65	1.95
center to		22.60	4.16	1.54	1.82
center, made	Acetone	37.49	4.82	2.00	2.36
of 0.51-mm		40.61	4.93	2.00	2.36
sheet brass					

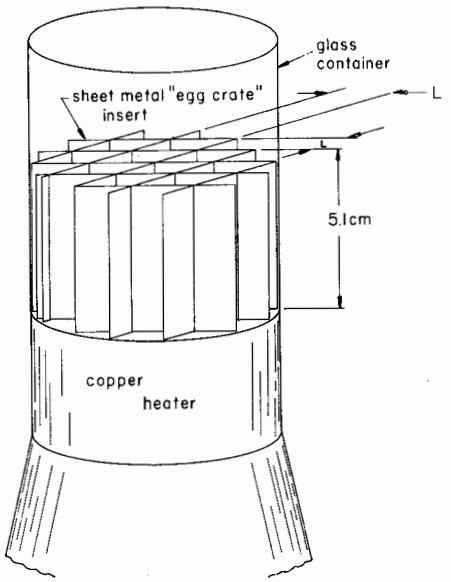

Fig. 10 Insert for augmenting q_{max}

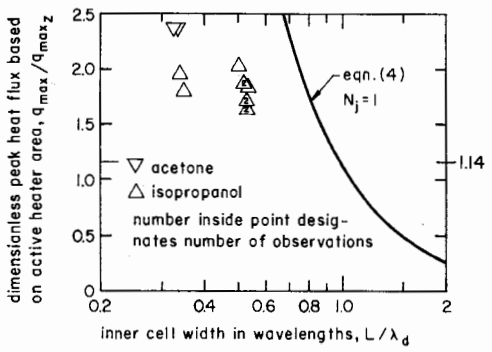

Fig. 11 Peak heat flux for a 6.35-cm-dia heater with an egg-crate structure above it (q_{max} based on active heater area)

pensate. Thus tabled values of q_{max}/q_{maxz} are given for both gross and the corrected surface area.

Fig. 11 shows the resulting corrected data in relation to the hydrodynamic theory. They fall a little low, in much the same way as did the data in Fig. 3. However, the data suggest that it is possible to roughly double the peak heat flux from a flat plate by inserting egg-crate structures. We suspect that these results could be slightly improved using a hexagonal (rather than square) array of walls in the structure since they would provide more nearly circular cells.

Conclusions

1 The peak pool boiling heat flux on an infinite flat plate is given by

$$\frac{q_{maxF}}{q_{maxZ}} = 1.14$$

2 If the plate is fewer than 3 wavelengths in width, the variation in q_{max}, as jets are added or removed, becomes very important. In this case:

$$\frac{q_{max}}{q_{maxZ}} = 1.14 \frac{N_j}{A_H/\lambda_d^2}$$

3 When N_j is equal to only one or two, the preceding equation can give rise to extremely large variations in q_{max}. This suggests that an egg-crate structure on a flat heater can be used to augment q_{max} significantly.

4 Experiments with appropriately sized egg-crate inserts show that it is possible to roughly double q_{max} over the infinite flat plate value.

References

1 Zuber, N., "Hydrodynamic Aspects of Boiling Heat Transfer," AEC Report No. AECU-4439, *Physics and Mathematics*, 1959.

2 Kutateladze, S. S., "On the Transition to Film Boiling Under Natural Convection," *Kotloturbostroenie*, No. 3, 1948, p. 10.

3 Lienhard, J. H., and Dhir, V. K., "Hydrodynamic Prediction of Peak Pool-Boiling Heat Fluxes From Finite Bodies," JOURNAL OF HEAT TRANSFER, TRANS. ASME, Series C, Vol. 95, No. 2, May 1973, pp. 152–158.

4 Sun, K. H., and Lienhard, J. H., "The Peak Pool Boiling Heat Flux on Horizontal Cylinders," *International Journal of Heat and Mass Transfer*, Vol. 13, 1970, pp. 1425–1439.

5 Bobrovich, G. I., Gogonin, I. I., and Kutateladze, S. S., "Influence of Size of Heater Surface on the Peak Pool Boiling Heat Flux," *Jour. Appl. Mech. and Tech. Phys.*, No. 4, 1964, pp. 137–138.

6 Lienhard, J. H., and Watanabe, K., "On Correlating the Peak and Minimum Boiling Heat Fluxes With Pressure and Heater Configuration," JOURNAL OF HEAT TRANSFER, TRANS. ASME, Series C, Vol. 88, No. 1, Feb. 1966, pp. 94–100.

7 Lienhard, J. H., "Interacting Effects of Gravity and Size Upon the Peak and Minimum Pool Boiling Heat Fluxes," NASA CR-1551, May 1970.

8 Cichelli, M. T., and Bonilla, C. F., "Heat Transfer to Liquids Boiling Under Pressure," *Trans. AIChE*, Vol. 41, 1945, p. 755.

9 Berenson, P. J., "Transition Boiling Heat Transfer From a Horizontal Surface," M.I.T. Heat Transfer Laboratory Technical Report No. 17, 1960.

10 Lienhard, J. H., and Keeling, K. B., Jr., "An Induced-Convection Effect Upon the Peak-Boiling Heat Flux," JOURNAL OF HEAT TRANSFER, TRANS. ASME, Series C, Vol. 92, No. 1, Feb. 1970, pp. 1–5.

11 Dhir, V. K., "Viscous Hydrodynamic Instability Theory of the Peak and Minimum Heat Fluxes," College of Engineering, Bulletin No. UKY-100, University of Kentucky, PhD dissertation, Nov. 1972.

12 Costello, C. P., Bock, C. O., and Nichols, C. C., "A Study of Induced Convective Effects on Pool Boiling Burnout," *CEP Symposium Series*, Vol. 61, 1965, pp. 271–280.

Reprinted from the November 1973 Journal of Heat Transfer